

# Investigation of Binary Element Reproduction Methods in Elemental Record Processes

Bohdana Havrysh<sup>1[0000-0003-3213-9747]</sup>, Oleksandr Tymchenko<sup>2[0000-0001-6315-9375]</sup>

Bohdan Kovalskyi<sup>1[0000-0002-5519-0759]</sup>, Myroslava Dubnevych<sup>1[0000-0001-7089-0190]</sup>

Orest Khamula<sup>1[0000-0003-0926-9156]</sup>, Michal Gregus<sup>3[0000-0002-8156-8962]</sup>

Mykola Logoyda<sup>4[0000-0001-7597-7973]</sup>

<sup>1</sup> Ukrainian Academy of Printing, Lviv, Ukraine

dana.havrysh@gmail.com, bkovalskyy@ukr.net,  
dubnevychmyroslava@gmail.com, khamula@gmail.com

<sup>2</sup> University of Warmia and Mazury, Olsztyn, Poland, o\_tymch@ukr.net

<sup>3</sup> Comenius University in Bratislava, Bratislava, Slovakia, Michal.Gregus@fm.uniba.sk

<sup>4</sup> Lviv Polytechnic National University, Lviv, Ukraine, mykola.m.lohoida@lpnu.ua

**Abstract.** We consider the methods of elemental recording of raster binary images on photographic or form material for systems of printing reproduction. In the process of tuning and comparing such processes, it is necessary to evaluate their sensitometric and structural-metric properties, which determine the quality of reproduction of the minimum image elements - raster points and strokes on the material carrier. The use of traditional sensitometry and structural analysis, which are used to calculate photographic processes, does not allow such a full assessment due to the difference between format and elemental recording methods, semitone and binary images, photographic and form materials. The peculiarities of the methods of reproduction of an image elements with elemental recording revealed to be expedient to be used at technological adjustment of printing reproduction system processes.

**Keywords:** binary images, optical density, printing forms, sampling, pixel functions.

## 1 Introduction and Problem Statement

The basic working properties of the image elements on the material carrier are determined by the gradation parameter. As a gradation parameter, optical density [1, 10] is often used to characterize the property of photographic forms to pass or delay radiation in the molding process, or the relative thickness of the printing layer. The register layer on the printing elements, which characterizes the property of printing forms to transfer ink in printing process [2]. For binary images, the gradation parameter has two levels - the upper  $l_u$  and the lower  $l_l$ , which, depending on the polarity of the pro-

cess, correspond to the active elements, purposefully formed radiation, and passive formed in the absence of radiation. If the active elements correspond to the lower level, then the process is positive (Fig. 1a), if to the upper one then the process is negative (Fig. 1b). The sensitometric curve (Fig. 1) shows the *threshold exposure*  $H_{thr}$  to which the basic working property of the passive image elements is provided, and the *minimum exposure*  $H_{min}$  from which the basic working property of the active elements is provided. If  $H_{min} = H_{thr}$  we get a threshold or step change in the gradation parameter.

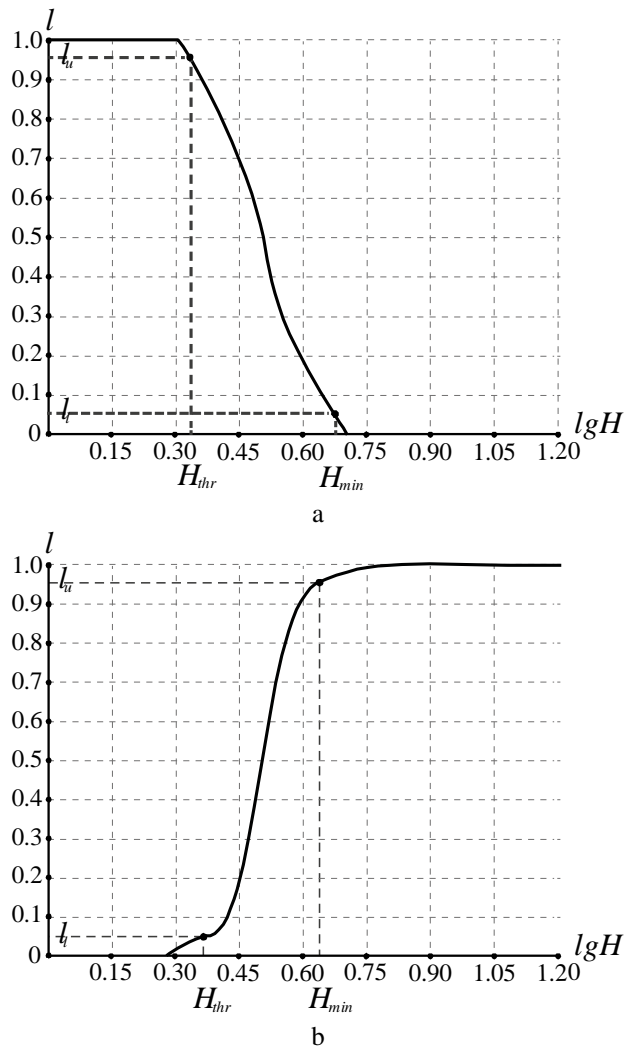


**Fig. 1.** Sensitometric curves of the elemental recording process: a - positive process; b - negative process

Sensitometric process curves will be used to identify the features of methods of reproducing image elements with elemental recording.

## 2 Development and Research of the Elemental Record Process Structure System

The basis of the developed system of structurometry of the elemental recording process is based on the normalized functions of distribution of effective energy density: for the pixel - the function of pixel reproduction (FPR) and for the edges of the energy plate - the boundary functions in the direction of personnel (BFP) and line scan (BFL) [3, 11].

Reproduction functions are functions of a discrete argument. We use the following notations:  $P(y, x)$  – for FPR and  $E^k(y)$  – for BFP. The  $x$  and  $y$  arguments related to the line and frame scans have a definition area [4]:

$$b : x, y = \{-b, -b + d, \dots, 0, \dots, b\}, \text{ where } d = \frac{1}{N} - \text{sampling step } N, b \in N.$$

Kernel Energy Density - The fraction of energy density in the center of the image element from the maximum level of the energy plate obtained while recording pixels in all positions, and pixel kernel functions - the dependence of the kernel energy density on the number of pixels forming active and passive elements,  $h_k^a(k)$  and  $h_k^p(k)$ . For the purpose of accuracy of estimation, it is advisable to use a balanced raster structure [5], for which on the matrix of balance points with recorded pixels, active raster points are formed, and unwritten ones form passive points, with points in light and dark regions being formed by identical and round shape pixels. For the balance structure, formulas for calculating the energy density of the kernel for k-pixel image elements can be written using FPR:

$$\begin{aligned} h_k^a(1) &= P(0,0), h_k^a(2) = 2P(0;0,5) \text{ etc.} \\ h_k^p(k) &= h_d(y'_c, y'_c) - h_k^a(k) \end{aligned} \quad (1)$$

where  $h_d(y'_c, y'_c)$  – the level of the energy plate at a point corresponding to the center of the image element. Formulas (1) show that the energy density of the nucleus is completely determined by the central part of the FPR within the sweep step.

## 3 Binary Images Reproduction Research

*Reproducing extended image elements.*

Depending on the FPR, a constant unit level or periodic oscillations of the energy density level in the direction and with the step of the frame scan can be formed on the energy plate (Fig. 2). In this case, a maximum is formed in integer coordinates  $h_d^{\max} = 1$  (rationing to the maximum), and in half offset coordinates, – minium  $h_{\min}$  (Fig. 2, b). The average level of energy density on the plate is equal to that specified

in the exposure system  $H_w$ , then, in the transition from relative values to absolute values for the minimum and maximum, we can write:  $R_n h_d^{\min}$  and  $R_n H_w$ , where  $R_n = \frac{2}{1 + h_d^{\min}}$  – is the conversion factor to the average level. In the presence of oscillations it is necessary to distinguish two values for the threshold and minimum exposure - local and average. The first is related to the action of energy density in the maximum or minimum, the second - with the average value of the energy density on the plate and the exposure specified in the system.

For offset printing forms, the main working property of the whitespace elements is provided in the complete absence of the printing layer ( $l_t = 0$ ), and printing elements at full thickness ( $l_u = 1$ ) [6]. Then the main working property of passive elements with exposure increasing begins to break at the maximums in which the energy density operates at  $H_{thr}^{loc}$ , with system exposure  $H_{thr}$ :

$$H_{thr}^{loc} = R_n H_{thr} \quad (2)$$

The basic working property of the active elements will finally be reached in the lows in which the energy density operates at  $H_{\min}^{loc}$ , at exposure  $H_{\min}$ :

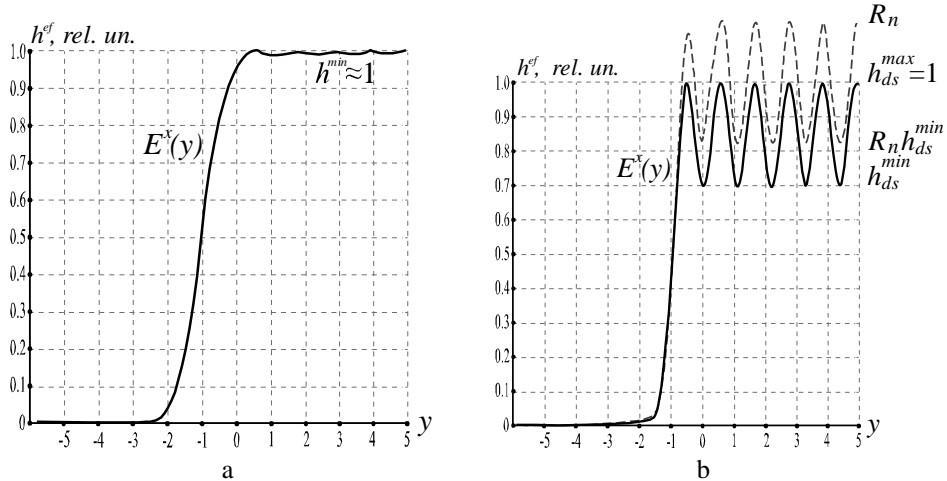


**Fig. 2.** Edge functions in the direction of the frame scan: a – constant level of the plate; b – plate level fluctuations

Exposure values  $H_{thr}$  and  $H_{\min}$  can be determined experimentally, but values  $H_{thr}^{loc}$  and  $H_{\min}^{loc}$  can be calculated by the formulas (2) and (3). With a constant unit level of the energy plate ( $h_d^{\min} = R_n = 1$ ) the exposure values set in the system are the same as the local values:  $H_{thr} = H_{thr}^{loc}$  and  $H_{\min} = H_{\min}^{loc}$ . As the amplitude of the oscillations increases  $R_n$  begins to increase and  $R_n h_d^{\min}$  decreases, then the threshold expo-

sure of  $H_{thr}$  is decreasing in relation to  $H_{thr}^{loc}$ , and the minimum exposure of  $H_{min}$  – is increasing in relation to the  $H_{min}^{loc}$ .

Starting with  $H_{min}$  the basic working properties of the long-lasting elements of the image will be provided, and this exposure can be considered to be minimally sufficient to reproduce them.

*Reproduction of small image elements.*

Image elements in the center of which the basic working property is provided are considered reproducible and form a pixel reproduction range of  $k^a \dots k^p$ , where  $k^a$  – is the number of recorded pixels that form the minimally reproduced active element of an image,  $k^p$  – is the number of unwritten pixels that form the minimally reproduced passive image element. The pixel reproduction range is related to the reproduction range of tone values [7], which is one of the basic parameters that determine the visual properties of printed product. The pixel width equals  $p - (k^a + k^p) + 1$ , where  $p$  – is the number of pixels in a raster cell, and increases with decrease of  $k^a + k^p$ .

We will investigate the factors that affect this amount and width of the range. In the center of the  $k$ -pixel active image element the energy density acts like this:  $h_k^a(k)R_nH_w$ , which for its reproduction should be not less than  $H_{min}^{loc}$ , then, considering (3) we can write the reproduction condition:

$$h_k^a(k) \geq h_{min} \text{ where } h_{min} = \frac{H_{min}^{loc}}{R_n H_w} = \frac{h_d^{min} H_{min}}{H_w} \quad (4)$$

In the center of  $k$ -pixel of the passive element, the image gives energy density  $h_k^p(k)R_nH_w$ , which should be smaller than  $H_{thr}^{loc}$  to recreate it, and considering (1) we can record the reproduction condition:

$$h_k^p(k) < h_{thr} \quad (5)$$

$$\text{where } h_{thr} = \frac{H_{thr}^{loc}}{R_n H_w} = \frac{H_{thr}}{H_w}$$

Analysis (4) and (5) shows that starting with  $H_{min}$  active and passive elements are reproduced,  $H_w = H_{min}$  – is the condition of the best reproduction of the passive elements and the worst active, and the increase of  $H_w$  comparatively to  $H_{min}$  improves the reproduction of the active and the reproduction of the passive elements.

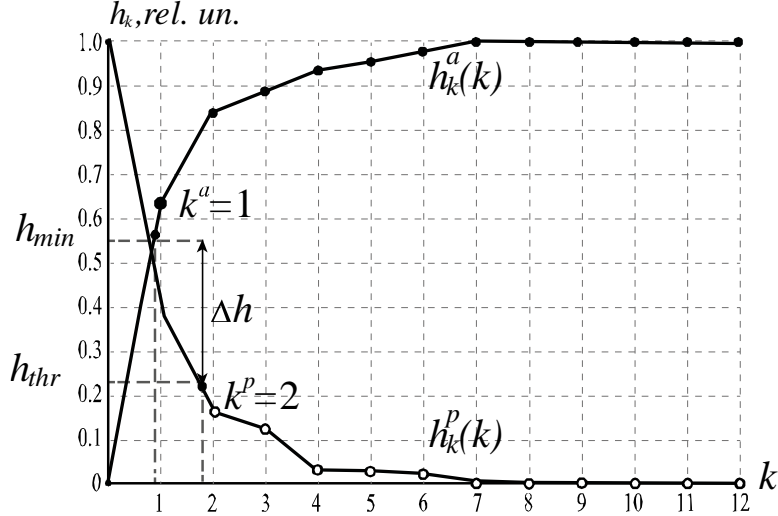


**Fig. 3.** Graphs of pixel functions

Let's consider the graphs of pixel functions for active  $h_k^a(k)$  and passive elements  $h_k^p(k)$ , which are piecewise linear, in one coordinate system (Fig. 3). The line  $h_{\min}$  at the intersection with the curve  $h_k^a(k)$  will give us the point whose abscissa, when rounded, is greater than the number of pixels  $k^a$ , that form the minimally reproduced active element. Similarly, the line  $h_{\thr}$  at the intersection with the curve  $h_k^p(k)$  gives us the point whose abscissa, when rounded to a greater number of pixels  $k^p$ , that form the minimally reproduced passive element.

Researching the influence of the values  $h_{\thr}$  and  $h_{\min}$ , *i.e.*  $h_{\thr}, h_{\min} \in [0,1]$  and  $h_{\thr} \leq h_{\min}$ , the sum of  $k^a + k^p$  allows us to draw the following conclusions.

- The value of  $k^a + k^p$  depends on the width of the interval  $\Delta h = h_{\min} - h_{\thr}$  and its position along the  $y$ -axis.
- The smaller the interval  $\Delta h$ , the smaller the sum of  $k^a + k^p$  and the wider the pixel recreation range.
- At a fixed value of the interval  $\Delta h$ , the minimum  $k^a + k^p$  corresponds approximately to its central position on the segment of the  $y$ -axis, *i.e.*  $h_{\min} + h_{\thr} = 1$  or  $H_w = H_{\thr} + h_d^{\min} H_{\min}$ . In this case, we obtain a symmetric pixel range with equal boundary values  $k^a = k^p$ . Some incertitude in the width of the range is introduced by the piecewise-linear nature of the functions, the angular coefficients of the linear sections of which depend on the FPR and the positions of the pixel recording.

- The maximum possible pixel reproducing range can be obtained when  $h_{\min} = h_{thr} = 0,5$ , which corresponds to the threshold sensitometric curve ( $H_{\min} = H_{thr}$ ). The maximum possible range for a given raster structure is completely determined by the central part of the FPR.
- Judging by (4) and (5)  $\Delta h \sim \frac{1}{H_w}$ , the interval narrows with increasing exposure in the system. However, as the exposure increases, the interval from the central position down the ordinate is shifted and  $k^a + k^p$  increases. As a result of these factors, in this case, the maximum range is asymmetrical with a smaller value of  $k^a$ .
- The piecewise linear nature of the pixel functions and the rounding of the pixels to integers results in the uncertainty of the bandwidth of up to two pixels. Also, the bandwidth is affected by the lower durability of the small printing elements not taken into account.

Let's investigate the effect of the nature of the FPR distribution on the reproduction of small image elements. In the analytical method of calculating FPR as a factor controlling the distribution proposed analytical method of calculating FPR. As a factor controlling the distribution of the energy density of the FPR, we take  $r_0$  – the laser beam radius in the area of constriction at the level  $e^{-2}$  at constant scattering parameters, selected to approximate the experimental data obtained for offset heat-sensitive plates [8].

As  $r_0$ , decreases, the energy density fraction in the central part of the FPR increases, the values of the pixel function  $h_k^a(k)$  increase accordingly, and the values  $h_k^p(k)$  decrease (table 1), increasing the pixel range to full ( $k^a = k^p = 1$ ). The energy density values in the center of the 1-pixel active and passive elements are calculated by (1), and by (4) and (5), we calculate the conditions for their reproduction and calculate the exposures from which these conditions are satisfied:

$$h_k^a(1) \geq \frac{H_{\min}^{loc}}{R_n H_w} \rightarrow H_w^{1a} \geq \frac{H_{\min}^{loc}}{R_n L(0,0)} \quad (6)$$

$$h_k^p(1) < \frac{H_{\min}^{loc}}{R_n H_w} \rightarrow H_w^{1n} < \frac{H_{\min}^{loc}}{R_n (1 - L(0,0))} \quad (7)$$

However, as  $r_0$  decreases, the amplitude of the oscillation level of the energy plate increases (columns  $h_d^{\min}$  and  $R_n$  of table 1), which can lead to the inadmissible partitioning of image elements into parts. The energy density at each point is formed by pixels that fall into the FPR definition area, and the minimals are formed in the coordinates of the frame sweep offset by half a step from the line item positions. Then the smallest value of the energy density is formed in the center of the 2-pixel element with the frame placement of pixels, for the calculation of which in formula (1) for the 2-pixel element with a row arrangement of pixels it is necessary to replace the argu-

ments of FPR:  $h_{\min}^a(2) = 2L(0,5; 0)$ . Starting with  $r_0 \approx 0,8$  the energy density at the center of such an element begins to fall (Table 1). From (4) we can calculate the condition of the integrity of the elements of the image and calculate the exposure at which this condition is satisfied:

$$h_{\min}^a(2) \geq \frac{H_{\min}^{loc}}{R_n H_w} \rightarrow H_w^{int} \geq \frac{H_{\min}^{loc}}{2R_n L(0,5; 0)} \quad (8)$$

**Table 1.** Influence of laser beam radius on image element reproduction.

$r_0$	$h_d^{\min}$	$R_n$	$h_k^a(1)$	$h_k^p(1)$	$h_{\min}^a(2)$	$\frac{H_{\min}^{loc}}{H_{\min}^{loc}}$	$\frac{H_{\min}^{loc}}{H_{\min}^{loc}}$	$\frac{H_w^{1a}}{H_{\min}^{loc}} \geq$	$\frac{H_w^{int}}{H_{\min}^{loc}} \geq$	$\frac{H_w^{1n}}{H_{\min}^{loc}} <$
1,20	1,00	1,00	0,37	0,63	0,53	1,00	1,00	2,72	1,89	1,58
1,10	0,99	1,00	0,42	0,58	0,57	1,00	1,00	2,36	1,73	1,73
1,00	0,98	1,01	0,49	0,51	0,62	0,99	1,01	2,02	1,60	1,94
0,90	0,94	1,03	0,57	0,43	0,64	0,97	1,03	1,71	1,51	2,25
0,80	0,87	1,07	0,65	0,35	0,64	0,94	1,07	1,43	1,46	2,70
0,70	0,75	1,14	0,74	0,26	0,59	0,87	1,17	1,18	1,48	3,35
0,60	0,57	1,27	0,81	0,19	0,48	0,79	1,37	0,97	1,63	4,20
0,50	0,37	1,46	0,87	0,13	0,32	0,68	1,87	0,78	2,11	5,28
<b>4×4</b>	<b>1,00</b>	<b>1,00</b>	<b>0,97</b>	<b>0,03</b>	<b>0,98</b>	<b>1,00</b>	<b>1,00</b>	<b>1,02</b>	<b>1,03</b>	<b>33,11</b>

It should be added that in the case of  $4 \times 4$ , a pixel consisting of 16 subpixels is used. With decreasing of  $r_0$  the exposure of  $H_w^{1a}$  decreases from which the 1-pixel active element is reproduced, and the exposure of  $H_w^{1p}$ , to which the 1-pixel passive element is reproduced (the table shows the ratio of  $H_w$  to local values). However, with  $r_0 \approx 0,8$  the minimum sufficient process exposure begins to be determined by the increased exposure of  $H_w^{int}$  integers required to maintain the integrity of the image elements (values highlighted in the table in bold). The need to increase exposure contradicts the lack of activity that is characteristic of, for example, the technology of elemental recording of offset printing forms. When using a pixel consisting of subpixels of a larger recording extension [9], a constant single level of the energy plate is formed, and the full pixel range is reached without increasing the exposure (row  $4 \times 4$  of the table). However, this approach requires specific hardware solutions.

## 4 Results and discussions

As a result of the researches the following features of reproduction of image elements in the processes of elemental recording were revealed:

- To obtain a larger pixel recreation range, the  $H_{thr}$  threshold and the minimum  $H_{min}$  exposure should be as close as possible to each other. The maximum possible range is reached in the case of a threshold sensitometric curve ( $H_{min} = H_{thr}$ ).
- Choosing a working exposure  $H_w$  in a system close to the minimum  $H_{min}$  results in poor reproduction of the active elements.
- The pixel range with equal lower and upper bounds is obtained at  $H_w = H_{thr} + h_d^{\min} H_{min}$ , but it is not maximal. The maximum pixel range is shifted toward larger exposures, with active elements reproducing better than passive ones. The result may be due to the lower resistance of small print elements to processing.
- The integrity of the image elements can be controlled in the center of a 2-pixel pixel element.
- Reducing the laser beam radius  $r_0$  allows us to obtain the full pixel range ( $k^a = k^p = 1$ ), but this increases the oscillation amplitude of the energy plate and, as a consequence: increases the minimum  $H_{min}$ , and decreases the threshold  $H_{thr}$  of the exposure; the integrity of the image elements is impaired and the condition of its preservation determines the minimum sufficient exposure in the system. This increases the working exposure in the system, which may be unacceptable with insufficient activity, which is characteristic, for example, for the technology of elemental recording of offset printing forms.
- The use of a pixel consisting of sub-pixels of greater recording expansion allows to obtain the full pixel range at a constant level of the power plate.

It is expedient to use the revealed features of reproduction of image elements when designing and technological tuning of processes with elemental recording.

## 5 Conclusion

Methods of elemental recording of bitmap raster images for photographic and form material for printing systems have been considered. The expediency of maximizing the minimum and maximum exposures with each other is shown, but the maximum pixel range is shifted toward larger exposures. To get the full pixel range, it is advisable to use sub-pixels and reduce the laser pro-radius.

## References

1. Wang, H-A.: Data hiding techniques for printed binary images. In: Proceedings International Conference on Information Technology: Coding and Computing, Las Vegas, NV, USA, 55-59 (2001)
2. Lall, P., et al.: Effect of Process Parameters on the Long-Run Print Consistency and Material Properties of Additively Printed Electronics. In: 2019 IEEE 69th Electronic Components and Technology Conference (ECTC), Las Vegas, NV, USA, 1347-1358 (2009) doi: 10.1109/ECTC.2019.00209
3. Zahir, S., and Naqvi, M.: A near minimum sparse pattern coding based scheme for binary image compression. In: IEEE International Conference on Image Processing 2005, Genova, 285-289 (2005) doi: 10.1109/ICIP.2005.1530048.
4. Das, P., Paul, K.C., Chatterjee, A.: Optimizing luminance and chrominance filtered channels by binary genetic algorithm (BGA) to generate color halftone image. In: 2015 Third International Conference on Image Information Processing (ICIIP), Waknaghat, 439-443 (2015) doi: 10.1109/ICIIP.2015.7414813.
5. Zhuge, X., Nakano, K.: An Error Diffusion Based Algorithm for Hiding an Image in Distinct Two Images. In: 2008 International Conference on Computer Science and Software Engineering, Hubei, 684-687 (2008) doi: 10.1109/CSSE.2008.335.
6. Wu, M., Liu, B.: Data hiding in binary image for authentication and annotation. IEEE Transactions on Multimedia, vol. 6, no. 4, 528-538, (2004) doi: 10.1109/TMM.2004.830814.
7. Chen, Y., Hsia, C., Tsai, Y., Chi, K.: Halftone-Based Data Hiding Method Using Orientation Modulation Strategy. In: 2018 1st International Cognitive Cities Conference (IC3), Okinawa, 192-194 (2018)
8. Shindo, Y., Kikuchi, N., Anada, K., Koka, S., Yaku, T.: Reduction of resolution for binary images by an octal grid graph representation model. In: 2013 IEEE/ACIS 12th International Conference on Computer and Information Science (ICIS), Niigata, 417-422 (2013) doi: 10.1109/ICIS.2013.6607876.
9. Shu, J., Hu, A., Meng, F., Meng, Y.: Improved binary codes for efficient content-based image retrieval. In: 2015 8th International Congress on Image and Signal Processing (CISP), Shenyang, 550-554 (2015) doi: 10.1109/CISP.2015.7407940.
10. Dronyuk, I., Nazarkevych, M., & Poplavská, Z.: Gabor filters generalization based on ateb-functions for information security. In International Conference on Man–Machine Interactions, 195-206, Springer, Cham (2017)
11. Peleshko, D., Rak, T., Peleshko, M., Izonin, I., Batyuk, D.: Two-frames image superresolution based on the aggregate divergence matrix. In: 2016 IEEE First International Conference on Data Stream Mining & Processing (DSMP), Lviv, 235-238 (2016) doi: 10.1109/DSMP.2016.7583548.